

Full Paper

Design, Synthesis, Molecular Docking, and Anticancer Activity of Phthalazine Derivatives as VEGFR-2 Inhibitors

Abdel-Ghany A. El-Helby¹, Rezk R. A. Ayyad^{1,2}, Helmy Sakr¹, Khaled El-Adl ¹, Mamdouh M. Ali³, and Fathalla Khedr¹

¹ Pharmaceutical Chemistry Department, Faculty of Pharmacy, Al-Azhar University, Cairo, Egypt

² Pharmaceutical Chemistry Department, Faculty of Pharmacy, Delta University, Gamasa, Dakahlia, Egypt

³ Biochemistry Department, Division of Genetic Engineering and Biotechnology, National Research Centre, Dokki, Giza, Egypt

Novel series of phthalazine derivatives **6–11** were designed, synthesized, and evaluated for their anticancer activity against two human tumor cell lines, HCT-116 human colon adenocarcinoma and MCF-7 breast cancer cells, targeting the VEGFR-2 enzyme. Compounds **7a,b** and **8b,c** showed the highest anticancer activities against both HCT116 human colon adenocarcinoma cells with IC₅₀ of 6.04 ± 0.30, 13.22 ± 0.22, 18 ± 0.20, and 35 ± 0.45 μM, respectively, and MCF-7 breast cancer cells with IC₅₀ of 8.8 ± 0.45, 17.9 ± 0.50, 25.2 ± 0.55, and 44.3 ± 0.49 μM, respectively, in comparison to sorafenib as reference drug with IC₅₀ of 5.47 ± 0.3 and 7.26 ± 0.3 μM, respectively. Eleven compounds in this series were further evaluated for their inhibitory activity against VEGFR-2, where compounds **7a**, **7b**, **8c**, and **8b** also showed the highest VEGFR-2 inhibition with IC₅₀ of 0.11 ± 0.01, 0.31 ± 0.03, 0.72 ± 0.08, and 0.91 ± 0.08 μM, respectively, in comparison to sorafenib as reference ligand with IC₅₀ of 0.1 ± 0.02. Furthermore, molecular docking studies were performed for all synthesized compounds to predict their binding pattern and affinity towards the VEGFR-2 active site, in order to rationalize their anticancer activity in a qualitative way.

Keywords: Anticancer agents / Molecular docking / Triazolo[3,4-a]phthalazine / VEGFR-2 inhibitors

Received: July 25, 2017; Revised: October 6, 2017; Accepted: October 10, 2017

DOI 10.1002/ardp.201700240



Additional supporting information may be found in the online version of this article at the publisher's web-site.

Introduction

The vascular endothelial growth factor (VEGF) signaling pathway plays pivotal role in regulating tumor angiogenesis. VEGF as a therapeutic target has been validated in various types of human cancers [1]. The VEGF receptor 2 (VEGFR-2) represents a major target within the angiogenesis-related kinases, hence considered the most important transducer of

VEGF-dependent angiogenesis [2]. Thus, inhibition of VEGF/VEGFR signaling pathway is regarded as an attractive therapeutic target for inhibition of tumor angiogenesis and subsequent tumor growth [3–5]. Phthalazin-1,4-diones have been reported as potent type II IMP dehydrogenase inhibitors and as effective anti-proliferative agents against different human and murine tumor cells particularly against hepatocellular carcinoma [4]. Moreover, 1,4-disubstituted phthalazines have attracted considerable attention as promising and effective anticancer agents [4, 5]. For example, 1-piperazinyl-4-substituted phthalazines have been reported as active cytotoxic agents against A549, HT-29, and MDAMB-231 [4]. Two studies reported the cytotoxicity of a series of 1-anilino-4-(arylsulfinyl/sulfonylmethyl)phthalazines against Bel-7402 (human liver cancer cell line) and HT-1080 (human fibrosarcoma cell line) [5].

Correspondence: Prof. Khaled El-Adl, Faculty of Pharmacy, Al-Azhar University, 1 Al-Mukhayam Al-Daem Str., 6th District, Nassr City, Cairo 00202-2262-5796, Egypt.

E-mail: eladlkhaled74@yahoo.com

Fax: 00202-2262-5796

During the last two decades there is a growing interest in the synthesis of several phthalazine derivatives for the treatment of cancer as potent inhibitors of VEGFR-2 [4–18]. Vatalanib (PTK787) was the first published anilino-phthalazine derivative as a potent VEGFR-2 inhibitor [14].

Sorafenib (Nexavar)[®] is a potent VEGFR-2 inhibitor and has been approved as antiangiogenic drug [19–21]. Regorafenib, the fluoro derivative of sorafenib, showed anti-proliferative activities on different cancer cell lines [22].

Based on the previous mentioned facts, we herein report the synthesis of new series of phthalazine derivatives 6–11 based on the triazolo[3,4-a]phthalazine scaffold, aiming to obtain potent VEGFR-2 inhibitors with good anticancer activity.

Results and discussion

Rationale and structure-based design

Study of the structure activity relationships (SAR) and common pharmacophoric features shared by sorafenib and various VEGFR-2 inhibitors revealed that most VEGFR-2 inhibitors shared four main features as shown in Fig. 1 [23–25]: (i) The core structure of most inhibitors consists of a flat heteroaromatic ring system that contains at least one N atom which occupied the catalytic ATP-binding domain; (ii) a central aryl ring (hydrophobic spacer), occupying the linker region between the ATP-binding domain and the DFG

domain of the enzyme [26]; (iii) a linker containing a functional group acting as pharmacophore (e.g., amino or urea) that possesses both H-bond acceptor and donor in order to bind with two crucial residues (Glu883 and Asp1044) in the DFG (Asp-Phe-Gly) motif, an essential tripeptide sequence in the active kinase domain. The NH motifs of the urea or amide moiety usually form one hydrogen bond with Glu883, whereas the C=O motif forms another hydrogen bond with Asp1044; and (iv) the terminal hydrophobic moiety of the inhibitors occupies the newly created allosteric hydrophobic pocket revealed when the phenylalanine residue of the DFG loop flips out of its lipophilic pocket defining DFG-out or inactive conformation. Thus, hydrophobic interactions are usually attained in this allosteric binding region [27]. Furthermore, analysis of the X-ray structure of various inhibitors bound to VEGFR-2 confirmed the sufficient space available for various substituents around the terminal heteroaromatic ring [28, 29].

The goal of our work was the synthesis of new agents with the same essential pharmacophoric features of the reported and clinically used VEGFR-2 inhibitors (e.g., sorafenib and vatalanib). The main core of our molecular design rationale comprised bioisosteric modification strategies of VEGFR-2 inhibitors at four different positions (Fig. 2).

Our target compounds were designed as triazolo[3,4-a]-phthalazine scaffold joined with different hydrophobic moieties through different linkers (HBA-HBD), the main pharmacophoric feature in VEGFR-2 inhibitors (e.g.,

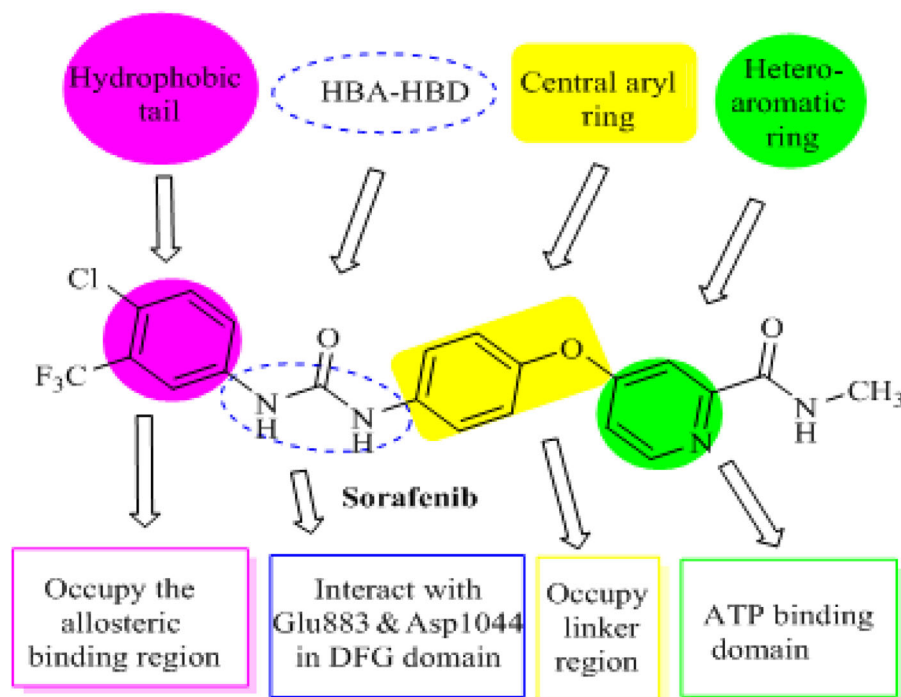


Figure 1. The basic structural requirements for sorafenib as reported VEGFR-2 inhibitor.

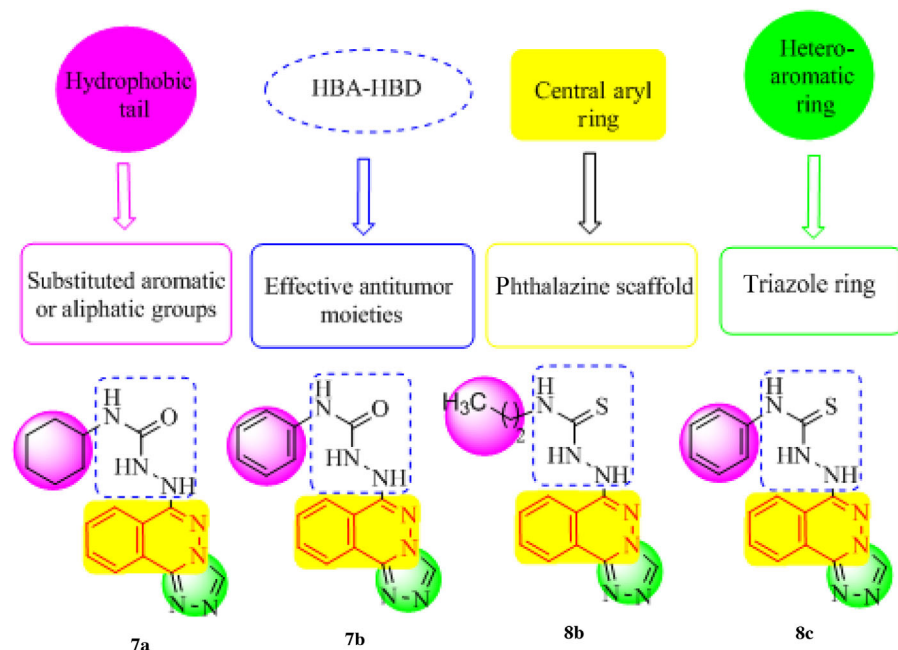


Figure 2. Summary for the possible modifications of VEGFR-2 inhibitors.

sorafenib) hoping to obtain more potent VEGFR-2 inhibitors. Firstly, bioisosteric approach was adopted in the target phthalazines, where triazole ring was selected to replace pyridine ring and phthalazine ring system to replace the central aryl ring of lead structures aiming to increase VEGFR-2 binding affinity. Then, different strategies were applied on this core. The first one depends on the utilization of different linkers, methylidenehydrazino linker ($-\text{NH}-\text{N}=\text{CH}-$) in the first series **6a–h**, hydrazinecarboxamide ($-\text{NH}-\text{NH}-\text{CO}-\text{NH}-$) in the second series **7a–b** and hydrazinecarbothioamide ($-\text{NH}-\text{NH}-\text{CS}-\text{NH}-$) in the third series **8a–c**, between triazolo[3,4-*a*]phthalazine and distal hydrophobic moieties. Also, the hydrophobic phenyl tail of the reported ligands was replaced by aliphatic groups namely cyclohexyl, ethyl, propyl, and methyl in compounds **7a**, **8a–b**, and **9**, respectively. The third strategy focused on the usage of different substituents on phenyl moiety as in compounds **6a–h**. Furthermore, the substitution pattern was selected to ensure different electronic and lipophilic environments which could influence the activity of the target compounds. On the other hand, the linkers in compounds **10** and **11** between distal phenyl moiety and the triazolo[3,4-*a*]phthalazine core was designed in different way, were they constitute a part of rigid ring structures to study the effect of free rotated open chain and/or closed ring structure linkers on SAR. These modifications were performed in order to carry out further elaboration of the phthalazine scaffold and to explore a valuable SAR. The designed target triazolo[3,4-*a*]phthalazines were synthesized to evaluate their potential VEGFR-2 inhibitory and anti-tumor activities against two human tumor cell lines, namely,

HCT-116 human colon adenocarcinoma and MCF-7 breast cancer.

The essential pharmacophoric features in the triazolo[3,4-*a*]phthalazine VEGFR-2 inhibitors [30, 31] include (Fig. 3): the presence of fused aromatic system represented by phthalazine ring as hydrophobic portion linked to different (un)substituted hydrophobic through different linkers which interacting as H-bond donor through its NH with the side chain carboxylate of the essential amino acid residue Glutamate883 and through hydrophobic interaction with its (un)substituted hydrophobic moieties with the hydrophobic pocket lined with the hydrophobic side chains of Leucine1033, Cysteine917, Phenylalanine916, Glutamate915, Valine914, Valine897, Lysine866, and Alanine864. In addition, 1,2,4-triazolo moiety was designed to replace the pyridine moiety of the reference ligand sorafenib. Compound **7a** has NHNHCONH linker which resembles the urea linker of sorafenib and formed H-bond with the essential amino acid Glutamate883. It also has hydrophobic distal cyclohexyl moiety which increases the affinity toward VEGFR-2 by hydrophobic interactions. These interactions may explain the highest anticancer activity.

Our target compounds were designed as hybrid molecules. These molecules formed of triazolo[3,4-*a*]phthalazine ring system joined with different substituted moieties through different linkers offering various electronic and lipophilic environments to study their impact on the activity hoping to obtain more potent anticancer agents. Molecular docking studies were carried out to study the interaction of the newly synthesized compounds with VEGFR-2, their binding mode

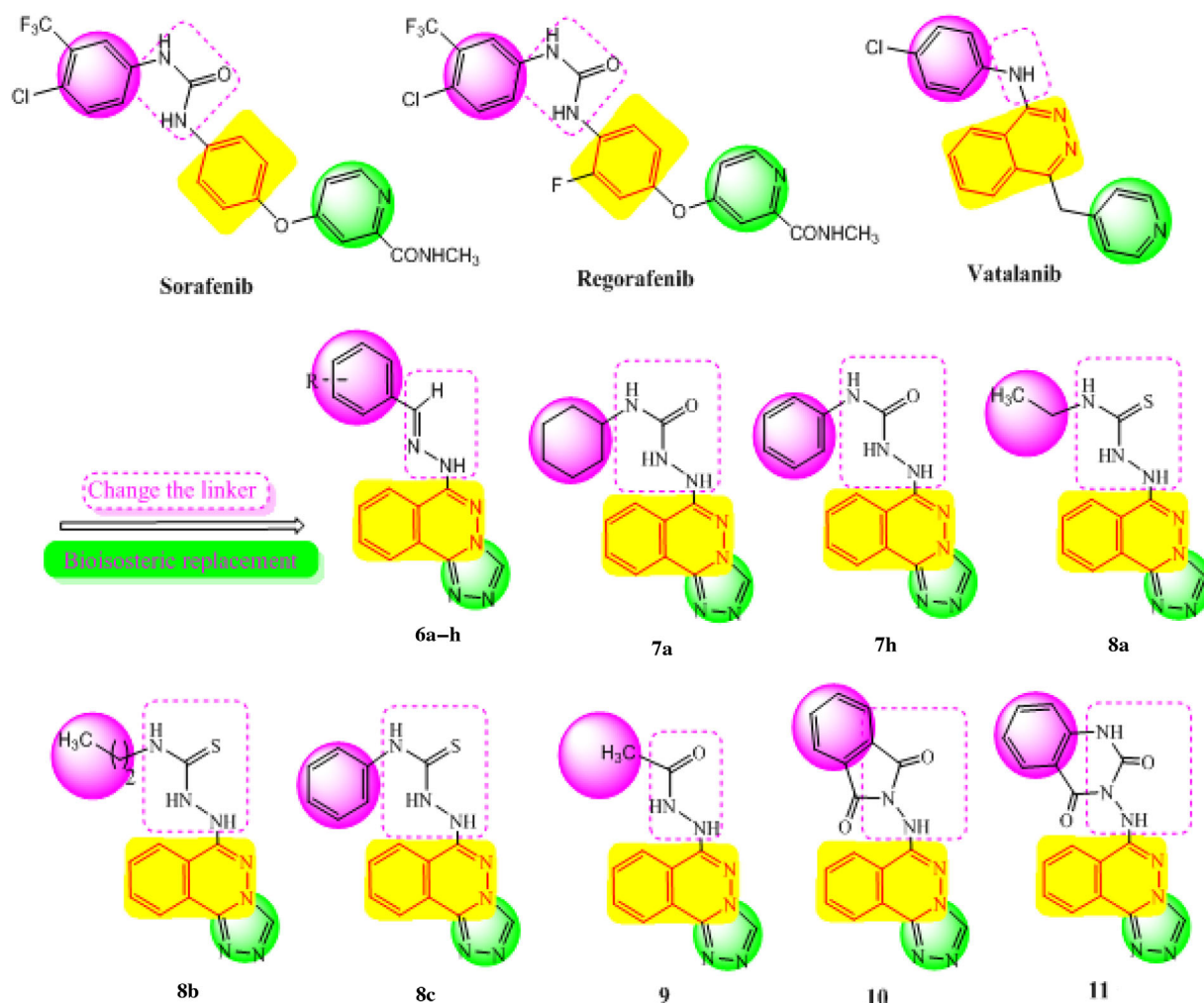


Figure 3. Structural similarities and pharmacophoric features of VEGFR-2 inhibitors and selected designed compounds.

and their ability to satisfy the pharmacophoric features required to induce the desired inhibition.

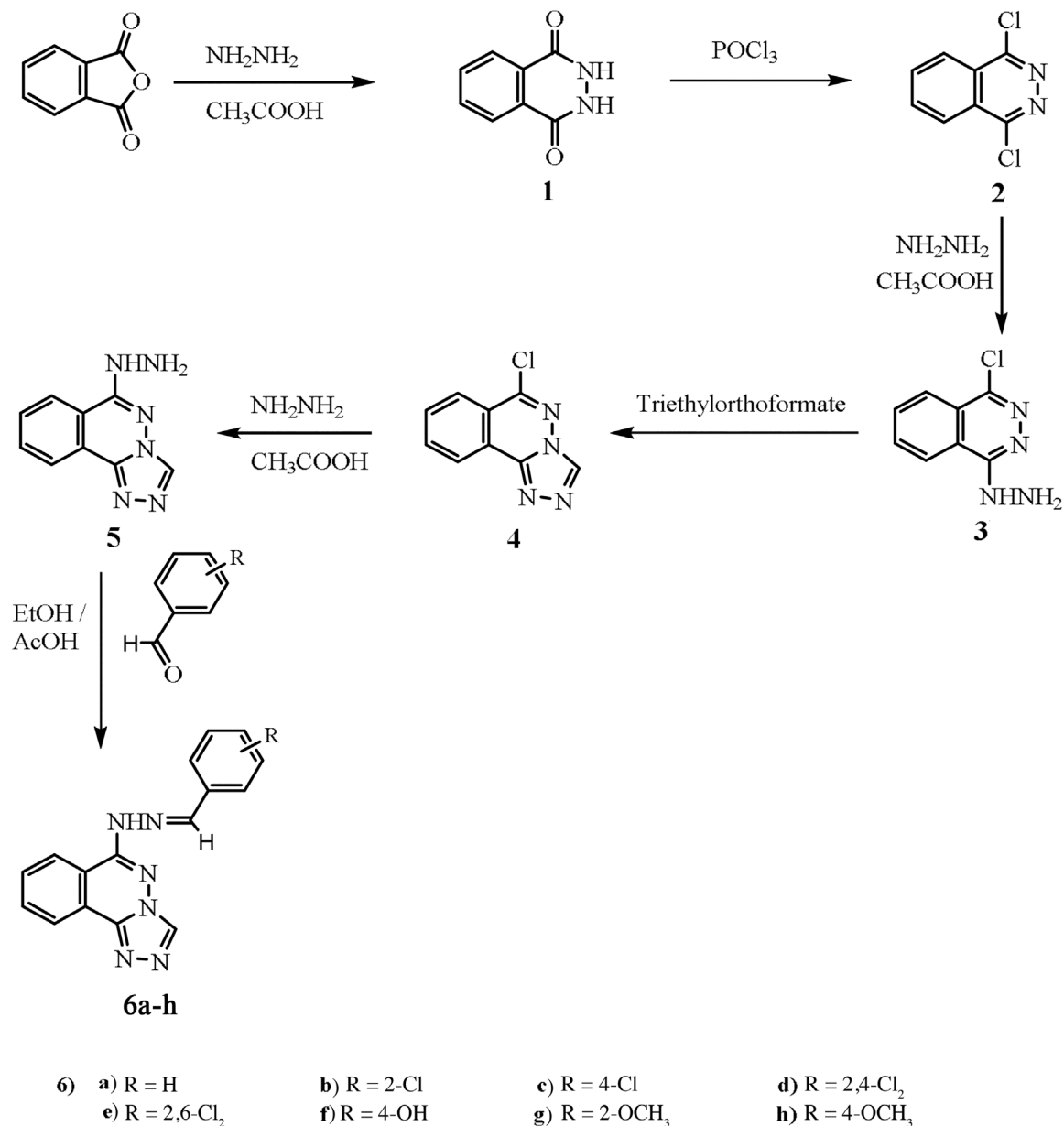
Chemistry

The synthetic strategy for preparation of the target compounds (5–11) is depicted in Schemes 1 and 2. Synthesis was initiated by reacting phthalic anhydride with hydrazine hydrate in the presence of acetic acid to provide 2,3-dihydrophthalazine-1,4-dione (1), which was treated with phosphorus oxychloride to afford 1,4-dichlorophthalazine (2). The obtained dichloro derivative 2 was refluxed with hydrazine hydrate in the presence of acetic acid to afford the corresponding 1-chloro-4-hydrazinylphthalazine (3). The key intermediate 6-chloro-[1,2,4]triazolo[3,4-a]phthalazine (4) was prepared via cyclization of 3 with triethylorthoformate. Heating the chloro intermediate 4 with hydrazine hydrate furnished the corresponding 6-hydrazinyl-[1,2,4]triazolo[3,4-a]phthalazine (5)

which underwent condensation with the appropriate aldehyde to obtain the corresponding Schiff's bases 6a–g (Scheme 1). The hydrazine derivative 5 was refluxed with the appropriate isocyanate and/or isothiocyanate to yield the corresponding carboxamide (7a,b) and/or carbothioamide (8a–c) derivatives, respectively, while when refluxed with acetic anhydride afforded the corresponding acetyl derivative 7. On the other hand, condensation of the hydrazine 5 with phthalic anhydride and/or isatoic anhydride furnished the corresponding isoindoline-1,3-dione (10) and/or quinazoline-2,4-dione (11) derivatives, respectively (Scheme 2).

Docking studies

In the present work, all modeling experiments were performed using Molsoft software. Each experiment used VEGFR-2 downloaded from the Brookhaven Protein Databank (PDB ID 1YWN) [30].

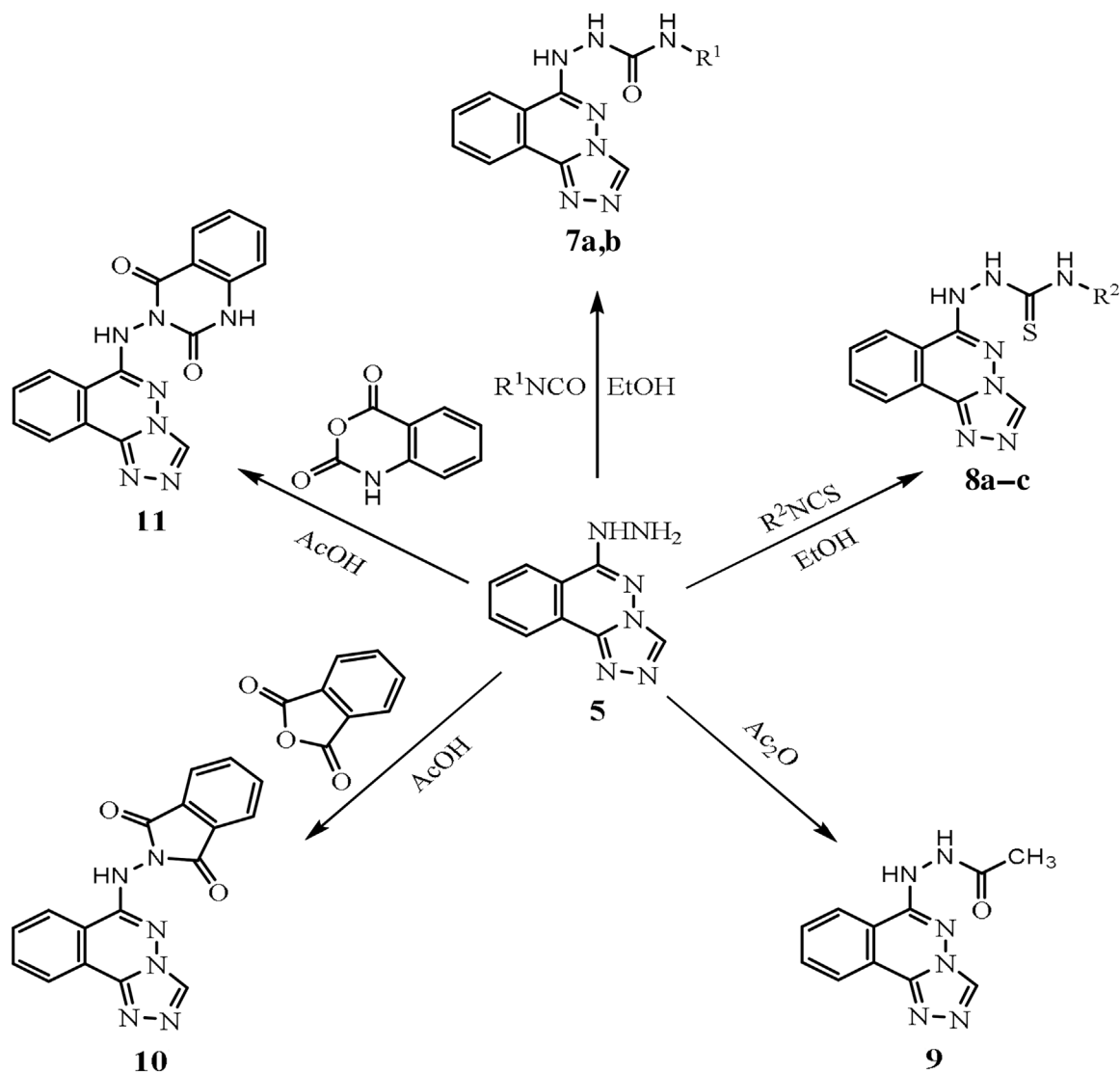


Scheme 1. Synthetic route for preparation of the target compounds **1** to **6a-h**.

The obtained results indicated that all studied ligands have similar position and orientation inside the putative binding site of VEGFR-2 which reveals a large space bounded by a membrane-binding domain which serves as entry channel for substrate to the active site (Fig. 4). In addition, the affinity of any small molecule can be considered as a unique tool in the field of drug design. There is a relationship between the affinity of organic molecules and the free energy of binding [32, 33]. This relationship can contribute in prediction and interpretation of the activity of the organic compounds

toward the specific target protein. The obtained results of the free energy of binding (ΔG) explained that most of these compounds had good binding affinity toward the receptor and the computed values reflected the overall trend (Table 1).

First, the molecular docking of **vatalanib** revealed affinity value of -73.26 kcal/mol and one H-bond with the key amino acid in the active site Glutamate883 (1.58 \AA) through its anilino nitrogen (NH linker). The phthalazine ring of vatalanib occupied the hydrophobic pocket formed by Glutamate883, Isoleucine886, Leucine887, and Aspartate1044. Moreover, the



- 7) a) $R^1 = C_6H_{11}$ b) $R = C_6H_5$
 8) a) $R^2 = C_2H_5$ b) $R = C_3H_7$ c) $R = C_6H_5$

Scheme 2. Synthetic route for preparation of the target compounds 7–11.

4-chlorophenyl moiety attached to the amino group at 1-position occupied the hydrophobic pocket formed by Cysteine1043, Aspartate1044, Valine897, Glutamate915, Valine914, Alanine864, and Lysine866. Furthermore, the pyridin-4-ylmethyl moiety at 4-position occupied the hydrophobic pocket formed by Valine897, Histidine892, Glycine891, and Isoleucine890 (Fig. 5).

The proposed binding mode of sorafenib revealed affinity value of -89.67 kcal/mol and four H-bonds. The urea linker formed two H-bonds with the key amino acid Glutamate883

(2.13 \AA) through its NH group and with Aspartate1044 (1.65 \AA) through its carbonyl group. The central phenyl ring occupied the hydrophobic pocket formed by Glutamate883, Isoleucine886, Leucine887, Isoleucine1042, Cysteine1043, and Aspartate1044. Moreover, the distal hydrophobic 3-trifluoromethyl-4-chlorophenyl moiety attached to the urea linker occupied the hydrophobic pocket formed by Cysteine1043, Leucine1033, Valine897, Valine914, Alanine864, Valine865, and Lysine866. Furthermore, the *N*-methylpicolinamide moiety occupied the hydrophobic groove formed by

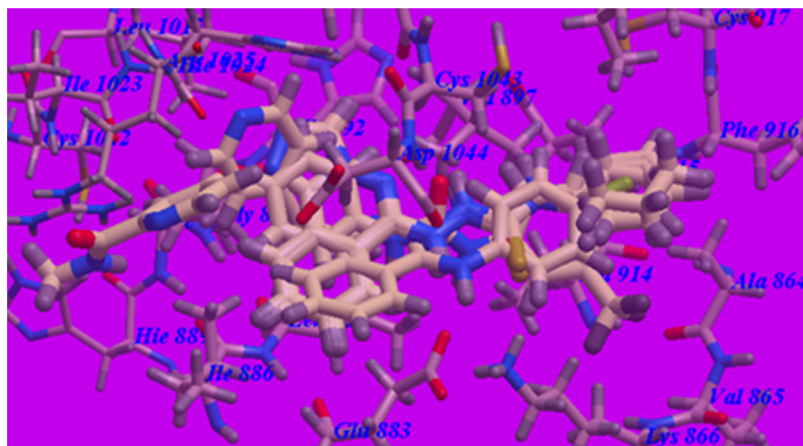


Figure 4. Superimposition of some docked compounds inside the binding pocket of 1WYN.

Table 1. The calculated ΔG (free energy of binding) and binding affinities for the ligands (ΔG in kcal/mol).

Compound	ΔG [kcal/mol]	Compound	ΔG [kcal/mol]
5	-66.67	7b	-80.97
6a	-71.84	8a	-69.56
6b	-74.23	8b	-77.53
6c	-75.65	8c	-79.32
6d	-74.53	9	-61.69
6e	-71.57	10	-59.95
6f	-72.79	11	-66.73
6g	-74.47	Vatalanib	-73.26
6h	-63.22	Sorafenib	-89.67
7a	-85.74		

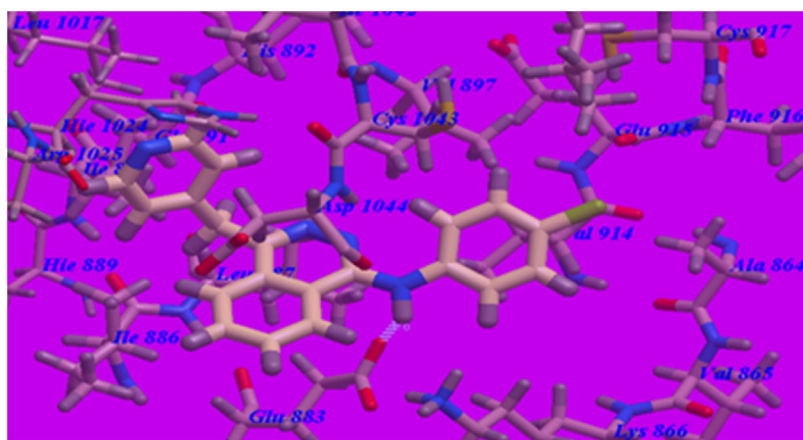


Figure 5. Predicted binding mode for vatalanib with 1WYN. H-bonded atoms are indicated by dotted lines.

Arginine1025, Histidine1024, Isoleucine1023, Cysteine1022, Leucine1017, Isoleucine890, Histidine889, and Isoleucine886 while its carbonyl was stabilized by formation of two H-bonds with Arginine1025 (1.90 and 2.12 Å) (Fig. 6). The linker played an important role in the binding affinity toward VEGFR-2 enzyme, where it was responsible for the higher binding

affinity of sorafenib than vatalanib. This finding encouraged us to use different linkers resembling that of sorafenib to obtain potent VEGFR-2 inhibitors.

As planned, the proposed binding mode of compound 7a is virtually the same as that of sorafenib which revealed affinity nearly equal to that of sorafenib with value of -85.74 kcal/

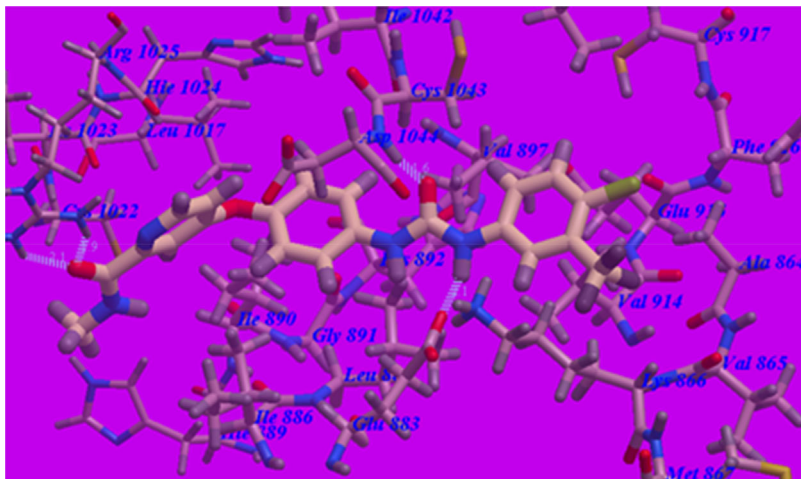


Figure 6. Predicted binding mode for sorafenib with 1WYN. H-bonded atoms are indicated by dotted lines.

mol and two H-bonds. Its NH group of the linker formed one H-bond with Glutamate883 (2.20 Å). The N atom at 5-position of 1,2,4-triazolo[3,4-a]phthalazine formed one H-bond with Aspartate1044 (2.46 Å). The 1,2,4-triazolo[3,4-a]phthalazine ring occupied the hydrophobic pocket formed by Aspartate1044, Cysteine1043, Isoleucine1042, Histidine1024, Cysteine1022, Leucine1017, Valine897, Isoleucine890, Leucine887, Isoleucine886, and Glutamate883. As a result of changing the NH linker by NHHCONH one, the cyclohexyl moiety attached to the new linker group at 6-position occupied the hydrophobic pocket formed by Leucine1033, Cysteine917, Phenylalanine916, Glutamate915, Valine914, Valine897, Lysine866, and Alanine864 (Fig. 7). These interactions of compound **7a** may explain the highest anticancer activity.

The proposed binding mode of **7b** (Fig. 8) is virtually the same as that of **7a** which revealed affinity value of -80.97 kcal/mol and two H-bonds with Glutamate883 (2.20 Å) and

Aspartate1044 (2.46 Å). The phenyl moiety occupied the same hydrophobic pocket occupied by cyclohexyl moiety of **7a**.

The proposed binding mode of **8c** is virtually the same as that of **7b** which revealed affinity value of -79.32 kcal/mol and two H-bonds with Glutamate883 (2.21 Å) and Aspartate1044 (2.41 Å) (Fig. 9).

Also, the proposed binding mode of **8b** (Fig. 10) is virtually the same as that of **7a** which revealed affinity value of -77.53 kcal/mol and two H-bonds with Glutamate883 (2.11 Å) and Aspartate1044 (2.47 Å). The propyl moiety occupied the same hydrophobic pocket occupied by cyclohexyl moiety of **7a**.

From the obtained docking results (Table 1), we concluded that NHHCONH and/or NHHCSNH linkers impart higher affinities toward VEGFR-2 enzyme than NH linker. The open chain free rotated linkers exhibited higher binding affinities than the rigid cyclic ones. C log P values or lipophilicity play an

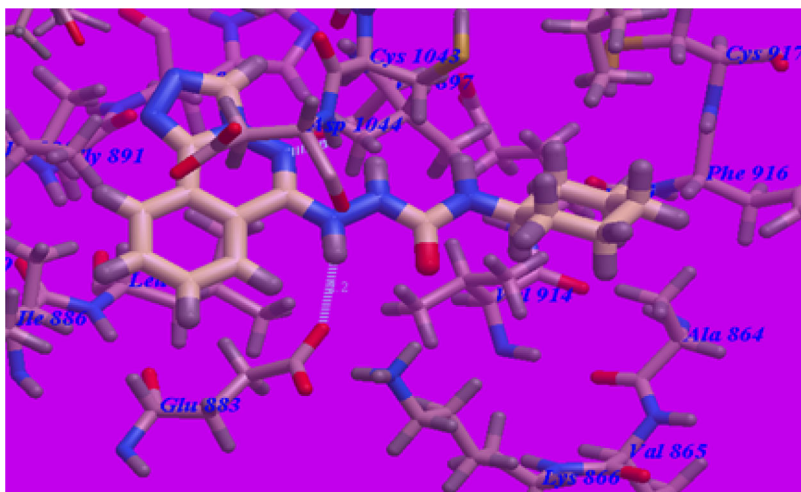


Figure 7. Predicted binding mode for **7a** with 1WYN.

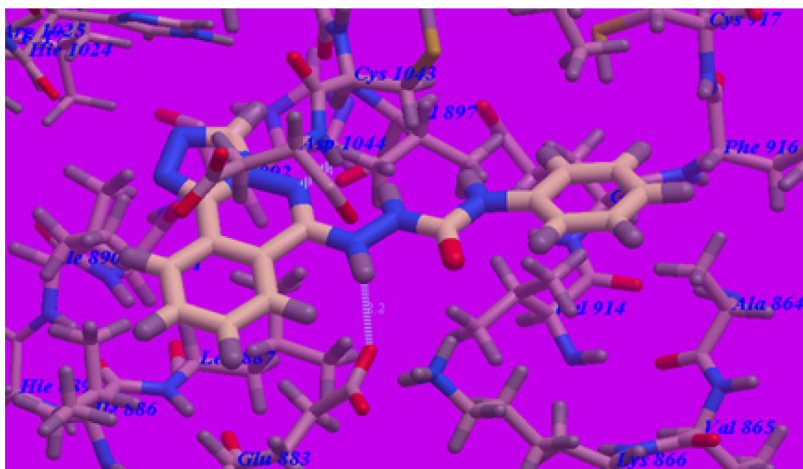


Figure 8. Predicted binding mode for 7b with 1WYN.

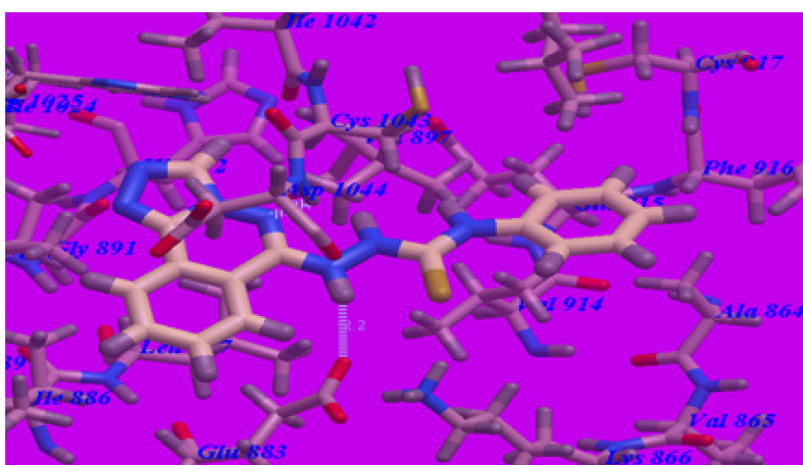


Figure 9. Predicted binding mode for 8c with 1WYN.

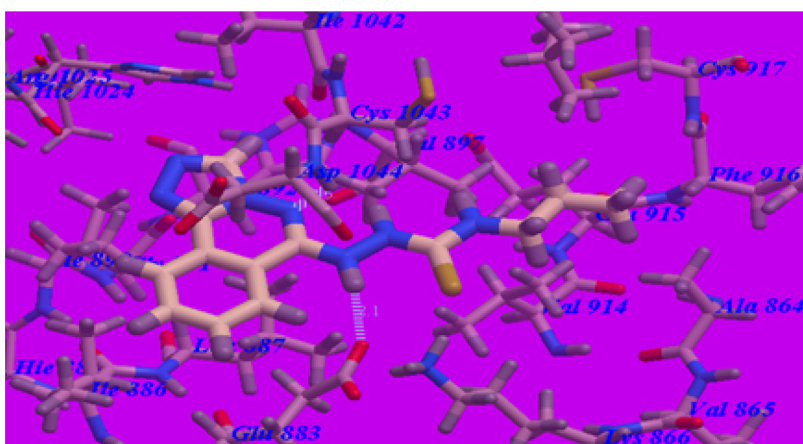


Figure 10. Predicted binding mode for 8b with 1WYN.

important role in their VEGFR-2 inhibitory activities which may be due to higher hydrophobic interactions.

Biological assays

In vitro cytotoxic activity

Anti-proliferative activity of the newly synthesized phthalazinones **6a–h** to **11** was examined in two human cancer cell lines, namely, HCT116 human colon adenocarcinoma and MCF-7 breast cancer using 3-[4,5-dimethylthiazol-2-yl]-2,5-diphenyltetrazolium bromide (MTT) colorimetric assay as described by Mosmann [34–36]. Sorafenib was included in the experiments as a reference cytotoxic drug. The results were expressed as growth inhibitory concentration (IC₅₀) values which represent the compound concentrations required to produce a 50% inhibition of cell growth after 72 h of incubation calculated from the concentration–inhibition response curve and summarized in Table 2. From the obtained results, it was explicated that most of the prepared compounds displayed excellent to modest growth inhibitory activity against the tested cancer cell lines. Investigations of the cytotoxic activity against HCT116 indicated that it was more sensitive cell line to the influence of the new derivatives. In particular, compound **7a** was found to be the most potent derivative of all the tested compounds against HCT116 and MCF-7 cancer cell lines with IC₅₀ = 6.04 ± 0.30 and 8.8 ± 0.45 μM, respectively. It has nearly the same activity as sorafenib against HCT116 (IC₅₀ = 5.47 ± 0.3) and MCF-7 cell lines (IC₅₀ = 7.26 ± 0.3 μM). With respect to the HCT116 human colon cancer, compounds **7b**, **8c**, and **8b** displayed good anticancer activity with IC₅₀ = 13.22 ± 0.22, 18 ± 0.20, and 35 ± 0.45 μM, respectively. Compounds **6c**, **6d**, and **6g** with IC₅₀ ranging from 110 ± 0.22 to 164 ± 1.27 μM displayed moderate cytotoxicity. Other compounds with IC₅₀ ranging from 178 ± 0.33 to 226.22 ± 2.43 μM exhibited low cytotoxicity.

Cytotoxicity evaluation in MCF-7 cell line revealed that compounds **7b**, **8c**, and **8b** with IC₅₀ = 17.9 ± 0.50, 25.2 ± 0.55, and 44.3 ± 0.49 μM, respectively, showed good cytotoxic

activity. Compounds **6d**, **6e**, and **6c** with IC₅₀ ranging from 140.4 ± 1.44 to 143.6 ± 1.32 μM showed moderate cytotoxicity. On the other hand, other compounds displayed low cytotoxicity.

In vitro VEGFR-2 kinase assay

The most active anti-proliferative derivatives **6a–g**, **7a–b**, and **8b–c** were selected to evaluate their inhibitory activities against VEGFR-2 by use of an anti-phosphotyrosine antibody with the Alpha Screen system (PerkinElmer, USA). The results were reported as a 50% inhibition concentration value (IC₅₀) calculated from the concentration–inhibition response curve and summarized in Table 2. Sorafenib was used as positive control in this assay. The tested compounds displayed good to moderate inhibitory activity with IC₅₀ values ranging from 0.11 to 1.55 μM. Among them, compound **7a** potently inhibited VEGFR-2 at low IC₅₀ value (0.11 ± 0.01 μM) equipotent as sorafenib IC₅₀ value (0.1 ± 0.02 μM). Also, compounds **7b**, **8c**, and **8b** possessed good VEGFR-2 inhibition with IC₅₀ values of 0.31 ± 0.03, 0.72 ± 0.08, and 0.91 ± 0.08 μM, respectively.

The preliminary SAR study has focused on the effect of replacement of the amino and urea linkers of vatalanib and sorafenib, respectively, with different linkers which interact as H-bond donor through its NH with the side chain carboxylate of the essential amino acid residue Glutamate883 and through hydrophobic interaction through its attached (un) substituted hydrophobic moieties. Also, replacement of pyridine moiety at position-4 of the phthalazine scaffold of the mentioned ligands by the fused 1,2,4-triazolo moiety of the synthesized compounds on the antitumor activities. 1,2,4-Triazolo moiety occupied the same hydrophobic pocket which is occupied by the pyridine moiety of the standard ligands. On the other hand different aliphatic groups were introduced instead of the phenyl moiety of the reference ligands. Moreover, different substitutions were introduced to the phenyl group with different lipophilicity and electronic nature in order to study their effect in the anticancer activity.

Table 2. *In vitro* cytotoxic activities of the newly synthesized compounds against HCT116 and MCF-7 cell lines.

Comp	IC ₅₀ (μM) ^{a)}			C log P	Comp	IC ₅₀ (μM) ^{a)}			C log P
	HCT116	MCF-7	VEGFR-2			HCT116	MCF-7	VEGFR-2	
6a	200.50 ± 2.24	NA ^{b)}	1.46 ± 0.16	2.78	7a	6.04 ± 0.30	8.8 ± 0.45	0.11 ± 0.01	2.66
6b	178 ± 0.33	253.5 ± 1.77	1.31 ± 0.14	3.41	7b	13.22 ± 0.22	17.9 ± 0.50	0.31 ± 0.03	2.46
6c	110 ± 0.22	143.6 ± 1.32	1.17 ± 0.13	3.46	8a	NA ^{b)}	NA ^{b)}	NT ^{c)}	–
6d	130.5 ± 0.26	140.4 ± 1.44	1.21 ± 0.12	4.07	8b	35 ± 0.45	44.3 ± 0.49	0.91 ± 0.08	2.18
6e	226.22 ± 2.43	142.3 ± 1.55	1.55 ± 0.16	4.04	8c	18 ± 0.20	25.2 ± 0.55	0.72 ± 0.08	2.36
6f	194.8 ± 0.22	NA ^{b)}	1.35 ± 0.14	2.31	11	NA ^{b)}	NA ^{b)}	NT ^{c)}	–
6g	164 ± 1.27	215.9 ± 1.63	1.29 ± 0.13	2.72	Sora.	5.47 ± 0.3	7.26 ± 0.3	0.10 ± 0.02	–
6h	NA ^{b)}	NA ^{b)}	NT ^{c)}	–					

Sora. = Sorafenib.

^{a)}IC₅₀ values are the mean ± S.D. of three separate experiments. ^{b)}NA: Compounds having IC₅₀ value >300 μM. ^{c)}NT: Compounds not tested for their VEGFR-2 inhibitory activity.

The data obtained revealed that the tested compounds displayed different levels of anticancer activity and possessed a distinctive pattern of selectivity against the HCT-116 human colon adenocarcinoma cell lines. Generally, the linkers, lipophilicity, and electronic nature exhibited an important role in anticancer activity. The NHHCONH and NHHCONH linkers as in compounds **7a–b** and **8b–c** were found to be essential for the good activity against both HCT116 human colon and MCF-7 breast cancer cell lines. The free rotating open chain NHHCONH linker exhibited higher activity than that of the cyclic NHHCONH one as in compound **11**. Alternatively, the distal phenyl group is not essential for activity where the more lipophilic cyclohexyl moiety as in compound **7a** displayed the highest anticancer potency against both cell lines. Also, the more lipophilic electron releasing cyclohexyl moiety as in compound **7a** exhibited higher anticancer activity than propyl as in **8b** and ethyl one as in **8a**. With respect to the HCT116 human colon cancer, the lipophilic electron deficient group Cl at *para*-position as compound **6c** exhibited higher potency than at *ortho*-position as **6b** which enables us to deduce that the lipophilic electron deficient group at *para*-position is essential for good activity. Also, electron deficient group (Cl) at *para*-position (e.g., **6c**) revealed higher activity than that of electron releasing groups (OH and OCH₃) as in **6f** and **6h**, respectively. On the other hand, electron releasing groups (OCH₃) at *ortho*-position as in **6g** showed higher activity than at *para*-position as **6h**. Furthermore, the mono Cl substitution at *para*-position (**6c**) showed higher activity than the 2,4- and 2,6-diCl substitution (as **6d** and **6e**, respectively). The activities were decreased in the order of **7a** > **7b** > **8c** > **8b** > **6c** > **6d** > **6g** > **6b** > **6f** > **6a** > **6e** for the colon cancer. With respect to the MCF-7 breast cancer, the lipophilicity played the major role in the activity. The lipophilic electron releasing aliphatic cyclohexyl moiety (at **7a**) showed higher activity than the phenyl (at **8c** and **7b**) which exhibited higher activity than the propyl moiety (at **8b**). The more lipophilic 2,4-diCl substitution at **6d** exhibited higher activity than 2,6-diCl at **6e** which displayed higher activity than the mono substitution 4-Cl and 2-Cl at **6c** and **6b**, respectively. Moreover, the electron releasing OCH₃ at *ortho*-position as **6g** revealed higher potency than the electron deficient one as **6b**. The activities were decreased in the order of **7a** > **7b** > **8c** > **8b** > **6d** > **6e** > **6c** > **6g** > **6b** for the breast cancer cells.

C log P correlation

As a trial for interpretation of the correlation between chemical structures of compounds **6a–g**, **7a–b**, and **8b–c** and their biological activity, an attempted correlation of anticancer activity with C log P data was calculated for the measurement of the lipophilicity factor which could be attributed in their anticancer activity. Determination of lipid-water partitioning *in vitro* is difficult, time-consuming, expensive, not always available, and not suitable to screen a large collection of new chemicals. Therefore, an alternative method was used based on computerized models [37]. So, the

C log P values were calculated for the new compounds to reflect the overall lipophilicity of these compounds and compared. The C log P data for all selected compounds are explained in Table 2 ranging from 2.18 to 4.07. Generally, it was found that the derivative with higher C log P value exhibited higher anticancer potency which may be explained by the hydrophobic interactions with active site of VEGFR-2 enzyme. From the structure of the synthesized compounds and the data shown in Table 2 we can divide these tested compounds into two groups. The first group is carboxamide and carbothioamide derivatives **7a–b** and **8b–c**, respectively. In this group, it is worthwhile to note that the higher potent compounds **7a**, **7b**, **8c**, and **8b** displayed their potency against both cell lines and as VEGFR-2 inhibitors according to their C log P order (C log P values of 2.66, 2.46, 2.36, and 2.18, respectively). The second group is the Schiff's bases **6a–g**. Among these compounds, **6d**, **6e**, **6c**, and **6b** with C log P values of 4.07, 4.04, 3.46, and 3.41, respectively, exhibited anticancer activity against MCF-7 breast cancer with good correlation with the lipophilicity factor. In spite of compound **6g** having higher anticancer potency than compound **6b**, it had lower C log P value (2.72) and had no correlation with the lipophilicity factor. In this group, the anticancer activity against HCT116 human colon cell lines and VEGFR-2 enzyme inhibition were affected by the electronic effect and had bad correlation with their lipophilicity factor.

Conclusion

The molecular design was performed to investigate the binding mode of the proposed compounds with VEGFR-2 receptor. The data obtained from the docking studies showed that compounds **7a**, **7b**, **8c**, and **8b** have considerable higher affinity toward the VEGFR-2 receptor in comparison to vatalanib as reference ligand and compound **7a** showed nearly the same affinity of sorafenib. This higher effect may be due to the change of the linker of vatalanib to resemble that of sorafenib. The data obtained from the biological screening fitted with that obtained from the molecular modeling. All the tested compounds showed variable anticancer activities. **7a**, **7b**, **8c**, and **8b** showed the highest anticancer activities against both HCT116 human colon adenocarcinoma with IC₅₀ of 6.04 ± 0.30, 13.22 ± 0.22, 18 ± 0.20, and 35 ± 0.45 μM, respectively, and MCF-7 breast cancer with IC₅₀ of 8.8 ± 0.45, 17.9 ± 0.50, 25.2 ± 0.55, and 44.3 ± 0.49 μM, respectively, compared to sorafenib as reference drug. Also, compounds **7a**, **7b**, **8c**, and **8b** showed the highest VEGFR-2 inhibition with IC₅₀ of 0.11 ± 0.01, 0.31 ± 0.03, 0.72 ± 0.08, and 0.91 ± 0.08 μM, respectively, in comparison to sorafenib as reference ligand. C log P values for the tested compounds play an important role in their anticancer potency especially against MCF-7 breast cancer. The obtained results showed that the most active compounds could be useful as a template for future design, optimization,

adaptation, and investigation to produce more potent and selective VEGFR-2 inhibitors with higher anticancer analogs.

Experimental

Chemistry

General

All melting points were determined by open capillary method on a Gallenkamp melting point apparatus at Faculty of Pharmacy Al-Azhar University and are uncorrected. The infrared spectra were recorded on Pye Unicam SP 1000 IR spectrophotometer at Pharmaceutical Analytical Unit, Faculty of Pharmacy, Al-Azhar University using potassium bromide disc technique. Proton magnetic resonance ^1H NMR spectra were recorded on a Mercury 300BB "NMR300" spectrometer at Faculty of Sciences, Cairo University, Cairo, Egypt. ^{13}C NMR spectra were recorded on an Agilent 400 MHz-NMR spectrometer at Chemical Laboratory – Ministry of Defense – Cairo. TMS was used as internal standard and chemical shifts were measured in δ scale (ppm). The mass spectra were carried out on Direct Probe Controller Inlet part to Single Quadropole mass analyzer in Thermo Scientific GCMS model ISQ LT using Thermo X-Calibur software at the Regional Center for Mycology and Biotechnology, Al-Azhar University. Elemental analyses (C, H, N) were performed on a CHN analyzer at Regional Center for Mycology and Biotechnology, Al-Azhar University. All compounds were within ± 0.4 of the theoretical values. The reactions were monitored by thin-layer chromatography (TLC) using TLC sheets precoated with UV fluorescent silica gel Merck 60 F254 plates and were visualized using UV lamp and different solvents as mobile phases.

The NMR spectra as well as the InChI codes of the investigated compounds together with some biological data are provided as Supporting Information.

Synthesis of compounds 1–4

2,3-Dihydrophthalazine-1,4-dione (**1**), 1,4-dichlorophthalazine (**2**), 1-chloro-4-hydrazinylphthalazine (**3**), and 6-chloro-[1,2,4]triazolo[3,4-a]phthalazine (**4**) were obtained according to the reported procedures [19].

6-Hydrazinyl-[1,2,4]triazolo[3,4-a]phthalazine (**5**)

6-Chloro-[1,2,4]triazolo[3,4-a]phthalazine (**4**) (2.046 g, 0.01 mol) was added to a boiling solution of hydrazine hydrate 70% (3.73 mL) in ethanol (50 mL). The reaction mixture was refluxed for 30 min, cooled and the resulting precipitate was filtered, washed with petroleum ether (2 \times 20 mL), dried and re-crystallized from ethanol to obtain compound **5**. Yield, 86%; m.p. 270–2°C; IR_{v,max} (cm⁻¹): 3447 (NH), 3224 (NH₂), 3081 (C–H aromatic), 2945 (C–H aliphatic), 1519 (C=N); ^1H NMR (400 MHz, DMSO-*d*₆): 4.40 (s, 2H, NH₂) (D₂O exchangeable), 7.79–7.84 (m, H, H-8 of phthalazine), 7.92–7.97 (m, H, H-9 of phthalazine), 8.27–8.30 (d, H, H-7 of phthalazine, *J* = 8.1 Hz), 8.41–8.44 (d, H, H-10 of phthalazine, *J* = 7.8 Hz), 8.99 (s, 1H, NH) (D₂O exchangeable), 9.15 (s, 1H, CH

of triazole ring); ^{13}C NMR (DMSO-*d*₆, 300 MHz): δ = 154.13 (C, C-6), 144.30 (C, C-10b), 136.14 (CH, C-3), 132.97 (CH, C-9), 132.41 (CH, C-8), 129.38 (CH, C-10), 125.73 (C, C-10a), 125.65 (CH, C-7), 124.97 (C, 6a); MS (*m/z*): 201 (M⁺+1, 7.75%), 200 (M⁺, 60.72%), 129 (96.18%), 102 (100%, base peak); Anal. calcd. for C₉H₈N₆ (m.w. 200): C, 53.99; H, 4.03; N, 41.98. Found: C, 54.17; H, 4.10; N, 41.99.

6-(2-(Substitutedbenzylidene)hydrazinyl)-[1,2,4]triazolo[3,4-a]phthalazine (**6a–h**)

General method: A mixture of 6-hydrazinyl-[1,2,4]triazolo[3,4-a]phthalazine (**5**) (0.4 g, 0.002 mol) and the appropriate aldehyde (0.002 mol) in absolute ethanol (30 mL) was refluxed for 6 h, in the presence of few drops of glacial acetic acid. The obtained solid product after cooling was filtered and recrystallized from ethanol to afford the corresponding Schiff's bases (**6a–h**), respectively.

6-(2-Benzylidenehydrazinyl)-[1,2,4]triazolo[3,4-a]phthalazine (**6a**)

Yield, 72%; m.p. 260–2°C; IR_{v,max} (cm⁻¹): 3211 (NH), 3070 (C–H aromatic), 2893 (C–H aliphatic), 1565 (C=N); ^{13}C NMR (DMSO-*d*₆, 400 MHz): δ = 159.74 (C, C-6), 150.11 (CH, NH=CH), 142.09 (C, C-10b), 140.20 (CH, C-3), 135.77 (C, C-1'), 134.98 (CH, C-9), 133.48 (CH, C-8), 132.24 (2CH, C-2' and C-6'), 128.78 (2CH, C-3' and C-5'), 126.95 (CH, C-4'), 125.95 (CH, C-10), 123.69 (C, C-10a), 123.40 (CH, C-7), 122.64 (C, 6a); MS (*m/z*): 289 (M⁺+1, 4.41%), 288 (M⁺, 17.73%), 185 (100%, base peak), 129 (81.04%); Anal. calcd. for C₁₆H₁₂N₆ (m.w. 288): C, 66.66; H, 4.20; N, 29.15. Found: C, 66.89; H, 4.24; N, 29.32.

6-(2-(2-Chlorobenzylidene)hydrazinyl)-[1,2,4]triazolo[3,4-a]phthalazine (**6b**)

Yield, 82%; m.p. 270–2°C; IR_{v,max} (cm⁻¹): 3185 (NH), 3074 (C–H aromatic), 2902 (C–H aliphatic), 1573 (C=N); ^1H NMR (300 MHz, DMSO-*d*₆): 7.41–7.54 (m, 3H, H-3, H-4, and H-5 of phenyl), 7.90–8.09 (m, 3H, H-6 of phenyl, H-8, and H-9 of phthalazine), 8.48–8.51 (m, 2H, H-7 and H-10 of phthalazine), 8.88 (s, 1H, N=CH), 9.32 (s, 1H, CH of triazole ring), 11.49 (s, 1H, NH) (D₂O exchangeable); Anal. calcd. for C₁₆H₁₁ClN₆ (m.w. 322.5): C, 59.54; H, 3.44; N, 26.04. Found: C, 59.70; H, 3.49; N, 26.18.

6-(2-(4-Chlorobenzylidene)hydrazinyl)-[1,2,4]triazolo[3,4-a]phthalazine (**6c**)

Yield, 84%; m.p. 267–9°C; IR_{v,max} (cm⁻¹): 3277 (NH), 3098 (C–H aromatic), 2948 (C–H aliphatic), 1565 (C=N); ^1H NMR (300 MHz, DMSO-*d*₆): 7.54–7.57 (m, 2H, H-3, and H-5 of phenyl), 7.79–7.82 (m, 2H, H-2, and H-6 of phenyl), 7.91–7.96 (m, H, H-8 of phthalazine), 8.00–8.05 (m, H, H-9 of phthalazine), 8.49–8.51 (m, 3H, H-7, and H-10 of phthalazine and N=CH), 9.31 (s, 1H, CH of triazole ring), 11.34 (s, 1H, NH) (D₂O exchangeable); Anal. calcd. for C₁₆H₁₁ClN₆ (m.w. 322.5): C, 59.54; H, 3.44; N, 26.04. Found: C, 59.67; H, 3.46; N, 26.21.

**6-(2-(2,4-Dichlorobenzylidene)hydrazinyl)-[1,2,4]-
triazolo[3,4-a]phthalazine (6d)**

Yield, 87%; m.p. 265–7°C; IR_{νmax} (cm⁻¹): 3157 (NH), 3091 (C–H aromatic), 2919 (C–H aliphatic), 1565 (C=N); ¹³C NMR (400 MHz, DMSO-d₆): δ = 161.09 (C, C-6), 149.21 (CH, NHN=CH), 146.35 (C, C-10b), 141.66 (CH, C-3), 140.03 (C, C-1'), 133.74 (CH, C-9), 130.96 (CH, C-8), 128.92 (2C, 2CCI), 127.53 (CH, C-3'), 124.88 (CH, C-10), 123.77 (C, C-10a), 123.31 (CH, C-7), 118.24 (C, 6a), 114.82 (2CH, C-5', and C-6'); MS (m/z): 361 (M⁺+4, 0.83%), 360 (M⁺+2, 1.67%), 359 (M⁺+2, 4.49%), 357 (M⁺, 7.98%), 185 (100%, base peak), 129 (41.81%); Anal. calcd. for C₁₆H₁₀Cl₂N₆ (m.w. 357): C, 53.80; H, 2.82; N, 23.53. Found: C, 53.96; H, 2.84; N, 23.72.

**6-(2-(2,6-Dichlorobenzylidene)hydrazinyl)-[1,2,4]-
triazolo[3,4-a]phthalazine (6e)**

Yield, 88%; m.p. 266–8°C; IR_{νmax} (cm⁻¹): 3192 (NH), 3092 (C–H aromatic), 2902 (C–H aliphatic), 1565 (C=N); ¹H NMR (300 MHz, DMSO-d₆): 7.42–7.60 (m, 3H, H-3, H-4, and H-5 of phenyl), 7.91–7.96 (m, H, H-8 of phthalazine), 8.01–8.06 (m, H, H-9 of phthalazine), 8.50–8.56 (m, 2H, H-7, and H-10 of phthalazine), 8.65 (s, 1H, N=CH), 9.28 (s, 1H, CH of triazole ring), 11.57 (s, 1H, NH) (D₂O exchangeable); Anal. calcd. for C₁₆H₁₀Cl₂N₆ (m.w. 357): C, 53.80; H, 2.82; N, 23.53. Found: C, 54.04; H, 2.80; N, 23.67.

**6-(2-(4-Hydroxybenzylidene)hydrazinyl)-[1,2,4]-
triazolo[3,4-a]phthalazine (6f)**

Yield, 78%; m.p. 270–2°C; IR_{νmax} (cm⁻¹): 3223 (NH), 3084 (C–H aromatic), 2945 (C–H aliphatic), 1594 (C=N); ¹H NMR (300 MHz, DMSO-d₆): 6.86–6.88 (m, 2H, H-3, and H-5 of phenyl), 7.60–7.62 (m, 2H, H-2, and H-6 of phenyl), 7.89–7.92 (m, H, H-8 of phthalazine), 7.96–7.98 (m, H, H-9 of phthalazine), 8.39 (s, 1H, N=CH), 8.46–8.48 (m, 2H, H-7, and H-10 of phthalazine), 9.27 (s, 1H, CH of triazole ring), 9.90 (s, 1H, OH) (D₂O exchangeable), 11.02 (s, 1H, NH) (D₂O exchangeable); Anal. calcd. for C₁₆H₁₂N₆O (m.w. 304): C, 63.15; H, 3.97; N, 27.62. Found: C, 63.53; H, 3.95; N, 27.80.

**6-(2-(2-Methoxybenzylidene)hydrazinyl)-[1,2,4]-
triazolo[3,4-a]phthalazine (6g)**

Yield, 76%; m.p. 271–3°C; IR_{νmax} (cm⁻¹): 3226 (NH), 3085 (C–H aromatic), 2955 (C–H aliphatic), 1594 (C=N); ¹H NMR (300 MHz, DMSO-d₆): 3.90 (s, 3H, OCH₃), 7.03–7.08 (m, H, H-3 of phenyl), 7.11–7.14 (m, H, H-5 of phenyl), 7.39–7.44 (m, H, H-4 of phenyl), 7.89–8.03 (m, 3H, H-6 of phenyl, H-8 and H-9 of phthalazine), 8.48–8.53 (m, 2H, H-7, and H-10 of phthalazine), 8.85 (s, 1H, N=CH), 9.30 (s, 1H, CH of triazole ring), 11.26 (s, 1H, NH) (D₂O exchangeable); Anal. calcd. for C₁₇H₁₄N₆O (m.w. 318): C, 64.14; H, 4.43; N, 26.40. Found: C, 64.35; H, 4.49; N, 26.56.

**6-(2-(4-Methoxybenzylidene)hydrazinyl)-[1,2,4]-
triazolo[3,4-a]phthalazine (6h)**

Yield, 77%; m.p. 273–5°C; IR_{νmax} (cm⁻¹): 3226 (NH), 3084 (C–H aromatic), 2935 (C–H aliphatic), 1594 (C=N); ¹H NMR

(300 MHz, DMSO-d₆): 3.83 (s, 3H, OCH₃), 7.04–7.06 (m, 2H, H-3, and H-5 of phenyl), 7.71–7.74 (m, 2H, H-2, and H-6 of phenyl), 7.93 (m, H, H-8 of phthalazine), 8.02 (m, H, H-9 of phthalazine), 8.45–8.51 (m, 3H, H-7, and H-10 of phthalazine and N=CH), 9.30 (s, 1H, CH of triazole ring), 11.12 (s, 1H, NH) (D₂O exchangeable); Anal. calcd. for C₁₇H₁₄N₆O (m.w. 318): C, 64.14; H, 4.43; N, 26.40. Found: C, 64.29; H, 4.51; N, 26.59.

**2-([1,2,4]Triazolo[3,4-a]phthalazin-6-yl)-N-
substitutedhydrazine-1-carboxamide (7a,b)**

A mixture of the hydrazine (5) (0.4 g, 0.002 mol) and the appropriate isocyanate namely cyclohexyl and/or phenyl isocyanate (0.002 mol), was refluxed in ethanol (25 mL) for 4 h. The reaction mixture was cooled and the formed solid was filtered and re-crystallized from ethanol to obtain compounds 7a,b, respectively.

**2-([1,2,4]Triazolo[3,4-a]phthalazin-6-yl)-N-
cyclohexylhydrazine-1-carboxamide (7a)**

Yield, 83%; m.p. 274–6°C; IR_{νmax} (cm⁻¹): 3289 (3NH overlapped), 3055 (C–H aromatic), 2927 (C–H aliphatic), 1627 (C=O), 1579 (C=N); ¹H NMR (300 MHz, DMSO-d₆): 1.18–1.23 (m, 4H, C-3, and C-5 cyclohexyl), 1.62 (m, 2H, C-4 cyclohexyl), 1.73–1.76 (m, 4H, C-2, and C-6 cyclohexyl), 3.40 (m, 1H, cyclohexyl), 5.91 (s, 1H, NH-cyclohexyl) (D₂O exchangeable), 7.79 (s, 1H, NH) (D₂O exchangeable), 7.85–7.87 (m, H, H-8 of phthalazine), 7.94–7.97 (m, H, H-9 of phthalazine), 8.33–8.36 (d, H, H-7 of phthalazine, J = 8.1 Hz), 8.43–8.45 (d, H, H-10 of phthalazine, J = 7.8 Hz), 9.18 (s, 1H, CH of triazole ring), 9.42 (s, 1H, NHCO) (D₂O exchangeable); Anal. calcd. for C₁₆H₁₉N₇O (m.w. 325): C, 59.06; H, 5.89; N, 30.13. Found: C, 59.18; H, 5.94; N, 30.37.

**2-([1,2,4]Triazolo[3,4-a]phthalazin-6-yl)-N-
phenylhydrazine-1-carboxamide (7b)**

Yield, 83%; m.p. 282–4°C; IR_{νmax} (cm⁻¹): 3226 (3NH overlapped), 3061 (C–H aromatic), 2930 (C–H aliphatic), 1635 (C=O), 1573 (C=N); ¹H NMR (300 MHz, DMSO-d₆): 7.21–7.26 (m, 1H, H-4 phenyl), 7.30–7.35 (m, 2H, H-3 and H-5 phenyl), 7.41–7.44 (m, 2H, H-2 and H-6 phenyl), 7.82–7.87 (m, H, H-8 of phthalazine), 7.88–7.97 (m, H, H-9 of phthalazine), 8.24–8.26 (d, H, H-7 of phthalazine, J = 8.7 Hz), 8.40–8.42 (d, H, H-10 of phthalazine, J = 8.4 Hz), 8.44 (s, 1H, NH) (D₂O exchangeable), 9.08 (s, 1H, CH of triazole ring), 9.66 (s, 1H, NHCO) (D₂O exchangeable), 10.21 (s, 1H, NH-phenyl) (D₂O exchangeable). MS (m/z): 320 (M⁺+1, 5.39%), 319 (M⁺, 9.96%), 119 (100%, base peak); Anal. calcd. for C₁₆H₁₃N₇O (m.w. 319): C, 60.18; H, 4.10; N, 30.70. Found: C, 60.43; H, 4.17; N, 30.85.

**2-([1,2,4]Triazolo[3,4-a]phthalazin-6-yl)-N-
substitutedhydrazine-1-carbothioamide (8a-c)**

A mixture of the hydrazine (5) (0.4 g, 0.002 mol) and the appropriate isothiocyanate, namely ethyl, propyl, and/or phenyl isothiocyanate (0.002 mol), was refluxed in ethanol (25 mL) for 6 h. the reaction mixture was cooled and the

formed solid was filtered and re-crystallized from ethanol to furnish compounds **8a–c**, respectively.

2-([1,2,4]Triazolo[3,4-a]phthalazin-6-yl)-N-ethylhydrazine-1-carbothioamide (8a)

Yield, 79%; m.p. 270–2°C; IR_{vmax} (cm⁻¹): 3254 (3NH overlapped), 3051 (C–H aromatic), 2902 (C–H aliphatic), 1523 (C=N); ¹H NMR (300 MHz, DMSO-d₆): 1.03–1.08 (t, 3H, CH₂CH₃), 3.43–3.50 (q, 2H, CH₂CH₃), 7.86–7.91 (m, H, **H-8** of phthalazine), 7.98–8.03 (m, H, **H-9** of phthalazine), 8.27 (s, 1H, NH-CH₂CH₃) (D₂O exchangeable), 8.30–8.33 (d, H, **H-7** of phthalazine, *J* = 8.7 Hz), 8.46–8.48 (d, H, **H-10** of phthalazine, *J* = 8.1 Hz), 9.30 (s, 1H, CH of triazole ring), 9.34 (s, 1H, NH) (D₂O exchangeable), 9.70 (s, 1H, NHCS) (D₂O exchangeable); Anal. calcd. for C₁₂H₁₃N₇S (m.w. 287): C, 50.16; H, 4.56; N, 34.12. Found: C, 50.39; H, 4.64; N, 34.37.

2-([1,2,4]Triazolo[3,4-a]phthalazin-6-yl)-N-propylhydrazine-1-carbothioamide (8b)

Yield, 81%; m.p. 280–2°C; IR_{vmax} (cm⁻¹): 3222 (3NH overlapped), 3064 (C–H aromatic), 2957 (C–H aliphatic), 1520 (C=N); ¹H NMR (300 MHz, DMSO-d₆): 0.78–0.83 (t, 3H, CH₂CH₃), 1.47–1.54 (m, 2H, CH₂CH₃), 3.37–3.43 (m, 2H, CH₂NH), 7.89–7.91 (m, H, **H-8** of phthalazine), 7.97–8.02 (m, H, **H-9** of phthalazine), 8.27 (s, 1H, NH-CH₂CH₃) (D₂O exchangeable), 8.30–8.33 (d, H, **H-7** of phthalazine, *J* = 8.1 Hz), 8.45–8.48 (d, H, **H-10** of phthalazine, *J* = 7.8 Hz), 9.28 (s, 1H, CH of triazole ring), 9.34 (s, 1H, NH) (D₂O exchangeable), 9.70 (s, 1H, NHCS) (D₂O exchangeable); Anal. calcd. for C₁₃H₁₅N₇S (m.w. 301): C, 51.81; H, 5.02; N, 32.53. Found: C, 52.06; H, 5.08; N, 32.46.

2-([1,2,4]Triazolo[3,4-a]phthalazin-6-yl)-N-phenylhydrazine-1-carbothioamide (8c)

Yield, 84%; m.p. 285–7°C; IR_{vmax} (cm⁻¹): 3208, 3124 (3NH overlapped), 3044 (C–H aromatic), 2902 (C–H aliphatic), 1594 (C=N); ¹³C NMR (400 MHz, DMSO-d₆): δ = 156.14 (C, C-6), 149.30 (C, CS), 141.72 (C, C-10b), 141.10 (C, C-1'), 140.07 (CH, C-3), 134.37 (CH, C-9), 133.10 (CH, C-8), 131.44 (CH, C-3'), 131.28 (CH, C-5'), 131.00 (CH, C-4'), 129.54 (2CH, C-2', and C-6'), 125.24 (CH, C-10), 123.90 (C, C-10a), 123.35 (CH, C-7), 118.09 (C-6a). MS (*m/z*): 335 (M⁺, 8.52%), 331 (9.56%), 200 (11.80%), 127 (100%, base peak); Anal. calcd. for C₁₆H₁₃N₇S (m.w. 335): C, 57.30; H, 3.91; N, 29.23. Found: C, 57.49; H, 3.95; N, 28.98.

N'-([1,2,4]Triazolo[3,4-a]phthalazin-6-yl)acetohydrazide (9)

The hydrazine derivative (**5**) (0.4 g, 0.002 mol) was refluxed with acetic anhydride (5 mL) for 3 h. The reaction mixture was allowed to attain room temperature and then poured carefully onto an ice-water (100 mL). The formed precipitate was filtered and crystallized from ethanol to give the target compound (**9**). Yield, 74%; m.p. 220–2°C; IR_{vmax} (cm⁻¹): 3237 (2NH overlapped), 3042 (C–H aromatic), 2919 (C–H aliphatic), 1666 (C=O), 1532 (C=N); ¹H NMR (300 MHz, DMSO-d₆): 2.00 (s, 3H, COCH₃), 7.84–7.90 (m, H, **H-8** of phthalazine), 7.96–8.01

(m, H, **H-9** of phthalazine), 8.34–8.37 (d, 3H, **H-7** of phthalazine, *J* = 8.1 Hz), 8.45–8.48 (d, H, **H-10** of phthalazine, *J* = 7.8 Hz), 9.20 (s, 1H, CH of triazole ring), 9.60 (s, 1H, NH) (D₂O exchangeable), 10.00 (s, 1H, NHCO) (D₂O exchangeable); MS (*m/z*): 242 (M⁺, 19.35%), 229 (6.89%), 210 (27.56%), 200 (15.04%), 128 (71.40%), 77 (100%, base peak); Anal. calcd. for C₁₁H₁₀N₆O (m.w. 242): C, 54.54; H, 4.16; N, 34.69. Found: C, 54.17; H, 4.10; N, 34.78.

2-([1,2,4]Triazolo[3,4-a]phthalazin-6-ylamino)-isoindoline-1,3-dione (10)

A mixture of the hydrazine (**5**) (0.4 g, 0.002 mol) and phthalic anhydride (0.30 g, 0.002 mol) was refluxed in glacial acetic acid (25 mL) for 6 h. The reaction mixture was allowed to attain room temperature, and then poured carefully onto crushed ice. The resulted solid precipitate was filtered, washed with water, and crystallized from ethanol to afford the target compound (**10**). Yield, 77%; m.p. 230–2°C; IR_{vmax} (cm⁻¹): 3222 (NH), 3055 (C–H aromatic), 2927 (C–H aliphatic), 1719 (C=O), 1527 (C=N); ¹H NMR (300 MHz, DMSO-d₆): 7.98–8.12 (m, 6H, **H-8**, and **H-9** of phthalazine and 4H of phenyl), 8.44–8.47 (d, H, **H-7** of phthalazine, *J* = 8.4 Hz), 8.52–8.55 (d, H, **H-10** of phthalazine, *J* = 7.8 Hz), 9.13 (s, 1H, CH of triazole ring), 10.69 (s, 1H, NH) (D₂O exchangeable); Anal. calcd. for C₁₇H₁₀N₆O₂ (m.w. 330): C, 61.82; H, 3.05; N, 25.44. Found: C, 61.98; H, 3.09; N, 25.61.

3-([1,2,4]Triazolo[3,4-a]phthalazin-6-ylamino)-quinazoline-2,4(1H,3H)-dione (11)

A mixture of the hydrazine (**5**) (0.4 g, 0.002 mol) and isatoic anhydride (0.33 g, 0.002 mol) was refluxed in glacial acetic acid (25 mL) for 12 h. The reaction mixture was allowed to attain room temperature, and then poured carefully onto crushed ice. The resulted solid precipitate was filtered, washed with water, and crystallized from ethanol to yield the target compound (**11**). Yield, 56%; m.p. 270–2°C; IR_{vmax} (cm⁻¹): 3222 (2NH overlapped), 3075 (C–H aromatic), 2935 (C–H aliphatic), 1646 (C=O), 1595 (C=N); ¹³C NMR (400 MHz, DMSO-d₆): δ = 162.62 (C, C-6), 159.56 (C, CON), 150.14 (C, CONH), 142.13 (C, C-10b), 140.22 (C, C-8'a), 135.79 (CH, C-3), 135.01 (CH, C-9), 133.50 (CH, C-7'), 132.27 (CH, C-8), 128.81 (CH, C-5'), 127.91 (CH, C-10), 126.98 (CH, C-6'), 125.98 (2C, C-10a, and C-4'a), 123.73 (CH, C-7), 123.42 (C, 6a), 122.68 (CH, C-8'); MS (*m/z*): 346 (M⁺+1, 1.09%), 345 (M⁺, 1.64%), 275 (45.20%), 102 (93.76%), 51 (100%, base peak); Anal. calcd. for C₁₇H₁₁N₇O₂ (m.w. 345): C, 59.13; H, 3.21; N, 28.39. Found: C, 59.42; H, 3.18; N, 28.46.

Docking studies

In the present work, all the target compounds were subjected to docking study to explore their binding mode toward VEGFR-2 enzyme. All modeling experiments were performed using molsoft program, which provides a unique set of tools for the modeling of protein/ligand interactions. It predicts how small flexible molecule such as substrates or drug candidates bind to a protein of known 3D structure

represented by grid interaction potentials (http://www.molsoft.com/icm_pro.html). Each experiment used the biological target VEGFR-2 downloaded from the Brookhaven Protein Databank (<http://www.rcsb.org/pdb/explore/explore.do?structureId=1YWN>). In order to qualify the docking results in terms of accuracy of the predicted binding conformations in comparison with the experimental procedure, the reported VEGFR-2 inhibitor drugs vatalanib and sorafenib were used as reference ligands.

Biological assays

In vitro cytotoxic activity

The cytotoxicity assays were performed at Pharmacology Department, Faculty of Pharmacy, Al-Azhar University, Cairo, Egypt. Cancer cells from different cancer cell lines, human colon adenocarcinoma (HCT116) and human breast adenocarcinoma (MCF7), were purchased from American Type Cell Culture Collection (ATCC, Manassas, USA) and grown on the appropriate growth medium (Roswell Park Memorial Institute medium (RPMI 1640)) supplemented with 100 mg/mL of streptomycin, 100 units/mL of penicillin and 10% of heat-inactivated fetal bovine serum in a humidified, 5% (v/v) CO₂ atmosphere at 37°C. Cytotoxicity assay by 3-[4,5-dimethylthiazole-2-yl]-2,5-diphenyltetrazolium bromide (MTT).

Exponentially growing cells from different cancer cell lines were trypsinized, counted, and seeded at the appropriate densities (2000–1000 cells/0.33 cm² well) into 96-well microtiter plates. Cells then were incubated in a humidified atmosphere at 37°C for 24 h. Then, cells were exposed to different concentrations of compounds (0.1, 10, 100, and 1000 μM) for 72 h. Then the viability of treated cells was determined using MTT technique as follows. Media were removed; cells were incubated with 200 μL of 5% MTT solution/well (Sigma–Aldrich, MO) and were allowed to metabolize the dye into colored-insoluble formazan crystals for 2 h. The remaining MTT solution were discarded from the wells and the formazan crystals were dissolved in 200 μL/well acidified isopropanol for 30 min, covered with aluminum foil and with continuous shaking using a MaxQ 2000 plate shaker (Thermo Fisher Scientific, Inc., MI) at room temperature. Absorbance was measured at 570 nm using a Stat FaxR 4200 plate reader (Awareness Technology, Inc., FL). The cell viability was expressed as percentage of control and the concentration that induces 50% of maximum inhibition of cell proliferation (IC₅₀) was determined using GraphPad Prism version 5 software (GraphPad software, Inc., CA) [34–36].

In vitro VEGFR-2 kinase assay

The kinase activity of VEGFR-2 was carried out in the National Research Centre, Giza, Egypt and measured by use of an anti-phosphotyrosine antibody with the Alpha Screen system (PerkinElmer, USA) according to manufacturer's instructions [6]. Enzyme reactions were performed in 50 mM Tris-HCl pH 7.5, 5 mM MnCl₂, 5 mM MgCl₂, 0.01% Tween-20 and 2 mM DTT, containing 10 μM ATP, 0.1 μg/mL biotinylated poly-GluTyr (4:1) and 0.1 nM of VEGFR-2 (Millipore, UK). Prior

to catalytic initiation with ATP, the tested compounds at final concentrations ranging from 0–2000 μg/mL and enzyme were incubated for 5 min at room temperature. The reactions were quenched by the addition of 25 μL of 100 mM EDTA, 10 μg/mL Alpha Screen streptavidine donor beads and 10 μg/mL acceptor beads in 62.5 mM HEPES pH 7.4, 250 mM NaCl, and 0.1% BSA. Plate was incubated in the dark overnight and then read by ELISA Reader (PerkinElmer). Wells containing the substrate and the enzyme without compounds were used as reaction control. Wells containing biotinylated poly-GluTyr (4:1) and enzyme without ATP were used as basal control. Percent inhibition was calculated by the comparison of compounds treated to control incubations. The concentration of the test compound causing 50% inhibition (IC₅₀) was calculated from the concentration–inhibition response curve (triplicate determinations) and the data were compared with sorafenib (Sigma–Aldrich) as standard VEGFR-2 inhibitor.

The authors extend their appreciation and thanks to Dr. Tamer Abdel-Ghany, Pharmacology & Toxicology Department, Faculty of Pharmacy, Al-Azhar University, Cairo, Egypt for helping in the pharmacological part.

The authors have declared no conflict of interest.

References

- [1] G. Niu, X. Chen, *Curr. Drug Targets* **2010**, *11*(8), 1000–1017.
- [2] K. Holmes, O. L. Roberts, A. M. Thomas, M. J. Cross, *Cell. Signal.* **2007**, *19*(10), 2003–2012.
- [3] S. Tugues, S. Koch, L. Gualandi, X. Li, L. Claesson-Welsh, *Mol. Aspects Med.* **2011**, *32*(2), 88–111.
- [4] W. M. Eldehna, H. S. Ibrahim, H. A. Abdel-Aziz, N. N. Farrag, M. M. Youssef, *Eur. J. Med. Chem.* **2015**, *89*, 549–560.
- [5] W. M. Eldehna, S. M. Abou-Seri, A. M. El Kerdawy, R. R. Ayyad, H. A. Ghabbour, M. M. Ali, D. A. Abou El Ella, *Eur. J. Med. Chem.* **2016**, *113*, 50–62. <https://doi.org/10.1016/j.ejmech.2016.02.029>
- [6] S. M. Abou-Seri, W. M. Eldehna, M. M. Ali, D. A. Abou El Ella, *Eur. J. Med. Chem.* **2015**, *107*, 165–179. <https://doi.org/10.1016/j.ejmech.2015.10.053>
- [7] M. I. Marzouk, S. A. Shaker, A. A. Abdel Hafiz, K. Z. El-Baghdady, *Biol. Pharm. Bull.* **2016**, *39*, 239–251.
- [8] T. L. Bush, M. Payton, S. Heller, G. Chung, K. Hanestad, J. B. Rottman, R. Loberg, G. Friberg, R. L. Kendall, D. Saffran, R. Radinsky, *Mol. Cancer Ther.* **2013**, *12*(11), 2356–2366. <https://doi.org/10.1158/1535-7163.MCT-12-1178>
- [9] C. J. Paller, M. D. Wissing, J. Mendonca, A. Sharma, E. Kim, H-S. Kim, M. S. Q. Kortenhorst, S. Gerber, M. Rosen, F. Shaikh, M. L. Zahurak, M. A. Rudek, H. Hammers, C. M. Rudin, M. A. Carducci, S. K. Kachhap, *Cancer Med.* **2014**, *3*(5), 1322–1335.

- [10] M. A. J. Duncton, E. L. P. Chekler, R. Katoch-Rouse, D. Sherman, W. C. Wong, L. M. Smith, J. K. Kawakami, A. S. Kiselyov, D. L. Milligan, C. Balagtas, Y. R. Hadari, Y. Wang, S. N. Patel, R. L. Rolster, J. R. Tonra, D. Surguladze, S. Mitelman, P. Kussie, P. Bohlen, J. F. Doody, *Bioorg. Med. Chem.* **2009**, *17*(2), 731–740.
- [11] M. A. J. Duncton, E. L. Piatnitski, R. Katoch-Rouse, L. M. Smith, A. S. Kiselyov, D. L. Milligan, C. Balagtas, W. C. Wong, J. Kawakamia, J. F. Doody, *Bioorg. Med. Chem. Lett.* **2006**, *16*(6), 1579–1581.
- [12] A. S. Kiselyov, V. V. Semenov, D. Milligan, *Chem. Biol. Drug Des.* **2006**, *68*, 308–313.
- [13] E. L. Piatnitski, M. A. J. Duncton, A. S. Kiselyov, R. Katoch-Rouse, D. Sherman, D. L. Milligan, C. Balagtas, W. C. Wong, J. Kawakamia, J. F. Doody, *Bioorg. Med. Chem. Lett.* **2005**, *15*(21), 4696–4698.
- [14] G. Bold, K.-H. Altmann, J. Frei, M. Lang, P. W. Manley, P. Traxler, B. Wietfeld, J. Brüggen, E. Buchdunger, R. Cozens, S. Ferrari, P. Furet, F. Hofmann, G. Martiny-Baron, J. Mestan, J. Rösel, M. Sills, D. Stover, F. Acemoglu, E. Boss, R. Emmenegger, L. Lässer, E. Masso, R. Roth, C. Schlachter, W. Vetterli, D. Wyss, J. M. Wood, *J. Med. Chem.* **2000**, *43*(12), 2310–2323.
- [15] J. Kankanala, A. M. Latham, A. P. Johnson, S. Homer-Vanniasinkam, C. W. G. Fishwick, S. Ponnambalam, *British J. Pharmacol.* **2012**, *166*, 737–748.
- [16] D.-Q. Xue, X.-Y. Zhang, C.-J. Wang, L.-Y. Ma, N. Zhu, P. He, K.-P. Shao, P.-J. Chen, Y.-F. Gu, X.-S. Zhang, C.-F. Wang, C.-H. Ji, Q.-R. Zhang, H.-M. Liu, *Eur. J. Med. Chem.* **2014**, *85*, 235–244.
- [17] E. N. Scott, G. Meinhardt, C. Jacques, D. Laurent, A. L. Thomas, *Expert Opin. Investig. Drugs* **2007**, *16*(3), 367–379.
- [18] K. M. Amin, F. F. Barsoum, F. M. Awadallah, N. E. Mohamed, *Eur. J. Med. Chem.* **2016**, *123*, 191–201. <https://doi.org/10.1016/j.ejmech.2016.07.049>
- [19] P. Wu, T. E. Nielsen, M. H. Clausen, *Trends Pharmacol. Sci.* **2015**, *36*(7), 422–439.
- [20] S. Wilhelm, C. Carter, M. Lynch, T. Lowinger, J. Dumas, R. A. Smith, B. Schwartz, R. Simantov, S. Kelley, *Nat. Rev. Drug Discov.* **2006**, *5*(10), 835–844.
- [21] A. Pircher, W. Hilbe, I. Heidegger, J. Dreves, A. Tichelli, M. Medinger, *Int. J. Mol. Sci.* **2011**, *12*(10), 7077–7099. <https://doi.org/10.3390/ijms12107077>
- [22] S. M. Wilhelm, J. Dumas, L. Adnane, M. Lynch, C. A. Carter, G. Schutz, K. H. Thierauch, D. Zopf, *Int. J. Cancer* **2011**, *129*(1), 245–255.
- [23] Q.-Q. Xie, H.-Z. Xie, J.-X. Ren, L.-L. Li, S.-Y. Yang, *J. Mol. Graph. Model.* **2009**, *27*(6), 751–758.
- [24] K. Lee, K.-W. Jeong, Y. Lee, J. Y. Song, M. S. Kim, G. S. Lee, Y. Kim, *Eur. J. Med. Chem.* **2010**, *45*(11), 542–547.
- [25] R. N. Eskander, K. S. Tewari, *Gynecol. Oncol.* **2014**, *132*(2), 496–505.
- [26] V. A. Machado, D. Peixoto, R. Costa, H. J. Froufe, R. C. Calhella, R. M. Abreu, I. C. Ferreira, R. Soares, M.-J. R. Queiroz, *Bioorg. Med. Chem.* **2015**, *23*(19), 6497–6509.
- [27] J. Dietrich, C. Hulme, L. H. Hurley, *Bioorg. Med. Chem.* **2010**, *18*(15), 5738–5748.
- [28] A. Garofalo, L. Goossens, P. Six, A. Lemoine, S. Ravez, A. Farce, P. Depreux, *Bioorg. Med. Chem. Lett.* **2011**, *21*(7), 2106–2112.
- [29] M. A. Aziz, R. A. Serya, D. S. Lasheen, A. K. Abdel-Aziz, A. Esmat, A. M. Mansour, A. N. B. Singab, K. A. Abouzid, *Sci. Rep.* **2016**, *6*(24460), 1–20. <https://doi.org/10.1038/srep24460>
- [30] S. A. H. El-Feky, H. A. Abd El-Fattah, N. A. Osman, M. Imran, M. N. Zedan, *J. Chem Pharm. Res.* **2015**, *7*(7), 1154–1166.
- [31] A. Papakyriakou, M. E. Katsarou, M. Belimezi, M. Karpusas, D. Vourloumis, *ChemMedChem.* **2010**, *5*, 18–129.
- [32] B. Baum, M. Mohamed, M. Zayed, C. Gerlach, A. Heine, D. Hangauer, G. Klebe, *J. Mol. Biol.* **2009**, *390*(1), 56–69.
- [33] L. Englert, A. Biela, M. Zayed, A. Heine, D. Hangauer, G. Klebe, *Biochim. Biophys. Acta* **2010**, *1800*, 1192–1202.
- [34] T. Mosmann, *J. Immunol. Methods* **1983**, *65*(1–2), 55–63.
- [35] D. A. Scudiero, R. H. Shoemaker, K. D. Paull, A. Monks, S. Tierney, T. H. Nofziger, M. J. Currens, D. Seniff, M. R. Boyd, *Cancer Res.* **1988**, *48*(17), 4827–4833.
- [36] F. M. Freimoser, C. A. Jakob, M. Aebi, U. Tuor, *Appl. Environ. Microbiol.* **1999**, *65*(8), 3727–3729.
- [37] A. A. El-Helby, R. R. A. Ayyad, K. El-Adl, H. Sakr, A. A. Abd-Elrahman, I. H. Eissa, A. Elwan, *Med. Chem. Res.* **2016**, *25*, 3030–3046.